A Minimal and Multi-Source Recording Setup for Ankle Joint Kinematics Estimation During Walking Using Only Proximal Information From Lower Limb

Rami Mobarak, *Graduate Student Member, IEEE*, Andrea Tigrini, *Member, IEEE*, Federica Verdini, *Member, IEEE*, Ali H. Al-Timemy, *Member, IEEE*, Sandro Fioretti, *Member, IEEE*, Laura Burattini, *Member, IEEE*, and Alessandro Mengarelli, *Member, IEEE*

***Abstract*— In this study, a minimal setup for the ankle joint kinematics estimation is proposed relying only on proximal information of the lower-limb, i.e. thigh muscles activity and joint kinematics. To this purpose, myoelectric activity of Rectus Femoris (RF), Biceps Femoris (BF), and Vastus Medialis (VM) were recorded by surface electromyography (sEMG) from six healthy subjects during unconstrained walking task. For each subject, the angular kinematics of hip and ankle joints were synchronously recorded with sEMG signal for a total of 288 gait cycles. Two feature sets were extracted from sEMG signals, i.e. time domain (TD) and wavelet (WT) and compared to have a compromise between the reliability and computational capacity, they were used for feeding three regression models, i.e. Artificial Neural Networks, Random Forest, and Least Squares - Support Vector Machine (LS-SVM). BF together with LS-SVM provided the best ankle angle estimation in both TD and WT domains (RMSE < 5.6 deg). The inclusion of Hip joint trajectory significantly enhanced the regression performances of the model (RMSE < 4.5 deg). Results showed the feasibility of estimating the ankle trajectory using only proximal and limited information from the lower limb which would maximize a potential transfemoral amputee user's comfortability while facing the challenge of having a small amount of information thus requiring robust data-driven models. These findings represent a significant step towards the development of a minimal setup useful for the control design of ankle active prosthetics and rehabilitative solutions.**

***Index Terms*— Surface electromyography, ankle joint, hip joint, least squares-support vector machine regression, kinematics estimation.**

Manuscript received 7 September 2023; revised 17 January 2024; accepted 3 February 2024. Date of publication 9 February 2024; date of current version 20 February 2024. This research has received funding from the project Vitality – Project Code ECS00000041, CUP I33C22001330007 - funded under the National Recovery and Resilience Plan (NRRP), Mission 4 Component 2 Investment 1.5 - 'Creation and strengthening of innovation ecosystems,' construction of 'territorial leaders in R&D' – Innovation Ecosystems - Project 'Innovation, digitalization and sustainability for the diffused economy in Central Italy – VITALITY' Call for tender No. 3277 of 30/12/2021, and Concession Decree No. 0001057.23-06-2022 of Italian Ministry of University funded by the European Union – NextGenerationEU. *(Rami Mobarak and Andrea Tigrini are co-first authors.) (Corresponding author: Alessandro Mengarelli.)*

This work involved human subjects or animals in its research. Approval of all ethical and experimental procedures and protocols was granted by the Institutional Ethics Committee of the Università Politecnica delle Marche, and performed in line with the Declaration of Helsinki.

Rami Mobarak, Andrea Tigrini, Federica Verdini, Sandro Fioretti, Laura Burattini, and Alessandro Mengarelli are with the Department of Information Engineering, Università Politecnica delle Marche, 60131 Ancona, Italy (e-mail: r.mobarak@pm.univpm.it; a.tigrini@staff.univpm.it; f.verdini@staff.univpm.it; s.fioretti@staff.univpm.it; l.burattini@staff.univpm.it; a.mengarelli@staff.univpm.it).

Ali H. Al-Timemy is with the Department of Biomedical Engineering, Al-Khwarizmi College of Engineering, University of Baghdad, Baghdad 10011, Iraq (e-mail: ali.altimemy@kecbu.uobaghdad.edu.iq).

Digital Object Identifier 10.1109/TNSRE.2024.3364976

I. Introduction

THE number of lower limb amputations alongside the reasons of amputations are variable around the world. Traumatic injuries are the leading cause of amputations in low and middle income countries while diabetes and peripheral vascular disease are more common in high income countries [1], [2]. Falls, roads accidents, and conflicts are the main reasons of traumatic injuries [2]. Unilateral lower limbs amputations are the most prevalent amputation level where the lower extremity roughly constitute around 90% of the new amputations [1], [3], [4], [5]. Transfemoral (TF) amputees form around 39% of the lower limbs amputations [4]. Therefore, literature highlights a persistent need to develop control strategies for lower limbs prosthesis that has to be adaptive with respect to the human intent of motion in order to restore the natural function of the amputees' lost leg [3], [6], [7]. To do this, possible solutions can be suggested by what was observed in exoskeletons control, where the information extracted from sensors placed on the lower limb was injected into the high-level control structures to provide modulated walking assistance to spinal cord injury or stroke patients [7], [8], [9], [10]. Such information can be extracted from signals as surface electromyography (sEMG) or mechanical sensors, that have been extensively used in the development of Human Machine Interfaces (HMI) [11], [12]. However, in a

real-world scenario, the sEMG is the most preferred signal to decode intended motion parameters such as locomotion pattern, joints angles, and torques, since sEMG precedes the development of the actual motion [13], [14], [15], [16], [17]. On the other hand, mechanical information appears as a result of the movement [18], [19]. Thus, even if systems based on mechanical information could provide accurate predictions, they might introduce a delay in the control of the prosthesis or exoskeleton, making the motion pattern unnatural [20], [21].

Two main kinds of strategies can be recognized in the literature to predict the intended motion. The first one involves the use of physical-based approaches as in [14], [22], [23], and [24]. Such strategy shows very challenging issues since it requires a description of complex physical relationships, even when few muscles or joints are considered in the control problem [14], [20]. The second strategy involves the use of data-driven modalities [15], [16], [25], [26], [27] that are advantageous since they allow to map the input signals into target variable, without the need for describing the complex relationship between the physical variables of interest [14]. The latter in turn is divided into two main subdivisions, i.e. classification and regression strategies. The former involves the prediction of a finite number of possible locomotion modes, eventually resulting in a not smooth movement patterns generation since a discrete decision-making system is adopted [13], [28], [29], [30]. Although classification based approaches showed the aforementioned issues, they demonstrated to be reliable in locomotion mode recognition so that they were largely employed in the practical context [3], [18]. However, while regression-based strategies were less exploited, they represent a viable solution in this field with respect to locomotion mode recognition since their final aim is the direct decoding of the input physiological signals into a continuous series of values of the target parameter [25], [26], [31], [32], [33], [34], [35], thus allowing smooth natural movement patterns, also without the computational burden required to tune physical based models [11]. For all these reasons, in this study, the problem of lower limb joint kinematics estimation was faced following the regression approach, completely driven by data.

Majority of the studies have employed the sEMG or mechanical based information in a separate fashion [11], [12], [15], [21], [28], [32], [36]. However, since sEMG and mechanical signals have their own contributions and barriers, possible solutions involved the fusion of sEMG and kinematic/kinetic information to support the natural sEMG predictive characteristic through the stability given by the mechanical information [3], [20]. In this context, different studies exploited the concept of fusing different sources of information to identify the lower limbs' locomotion modes as, for instance, level walking, stair ascent or descent [18], [30], [37], [38]. In [18] lower limbs locomotion modes for TF amputees were identified by feeding support vector machine (SVM) classifier with the myoelectric activity of up to eight residual thigh muscles and one 6 degrees of freedom (DOF) load cell, fixed on a prosthesis. Spanias et al. [37] faced the same problem by using sEMG data from eight probes, with twenty mechanical sensor channels, whereas in [38], an enhanced accuracy was obtained by fusing nine sEMG electrodes with thirteen inertial measurement units (IMU) from the leg prosthesis. Zhang and Huang [30] used eight sEMG channels information from the thigh muscles with one 6-DOF load cell fixed on a prosthetic pylon and two IMUs, fixed within the prosthetic socket for the purpose of task transition prediction of TF amputees. They also investigated the possibility of reducing the setup complexity while maintaining the desired performances and proposed a final reduced setup of four sEMG channels, one load cell and one IMU [30].

On the other hand, neuromuscular–mechanical fusion was less investigated under regression perspective. For instance, Gupta et al. [20] investigated the effect of adding knee trajectory to sEMG signals of the shank muscles, to estimate the ankle joint angle. They reported significant improvements made by the inclusion of mechanical information to the regression models. Although the proposed method provided promising results, it is not applicable for TF amputees since it is not possible to record the shank muscles sEMG or knee joint angle for them [7] and [39].

From the aforementioned studies, two different issues emerge as the main limitation in lower limb joint kinematics estimation for prosthetic control. Firstly, the high performances of the classification or regression models, achieved in the previous studies, were obtained at the expense of a large number of sensors placed over the human body. This eventually results in cumbersome setups that hamper the practical applicability of the proposed solutions in a daily usage scenario. This represents a well-acknowledged problem and in this view some efforts have been yet devoted for dealing with this issue, for instance, Keleş and Yucesoy [36] investigated the possibility of boosting the data-driven model performances for ankle joint angle estimation by fusing sEMG from non-functionally and functionally related muscles, concluding that it is possible to estimate the ankle angle trajectory using a combination of two thigh muscles and one shank muscle. Although a reduced sEMG setup was used, myoelectric information from the shank was still to be included [36], making the proposed solution not applicable for TF amputees. This limitation can be recognized also in other studies, that included IMU sensors placed on the shank for ankle joint angle estimation [12], [20], [27]. Hence, despite they may sound promising solutions for volitional lower limb joint angle estimation, they are not directly applicable for TF amputees. Hence, the estimation of ankle joint kinematics from the upper part of the lower limb represents the second main issue that deserves to be addressed in this field. In this context, it's also important to highlight the clinical value of a reliable ankle angle estimation approach if achieved, since this angular position can be used as a position control modality for active-ankle prostheses [40], particularly beneficial for individuals with limited influence over the ankle joint [41], such as an artificial ankle joint in TF amputees. An ankle position control approach, as highlighted in literature, plays a vital role in ensuring proper heel-strike during walking and facilitating foot clearance in the swing phase, emphasizing its crucial functional role in human locomotion aid [42].

Therefore, the purpose of the study was to estimate the flexion-extension ankle angle by relying only on information from proximal sources that can be available also in the case of a TF amputation. Thus, the first hypothesis was that a minimal sEMG setup, involving exclusively thigh muscles, can provide a reliable estimation of ankle angular kinematics. Moreover, the second hypothesis was that the introduction of kinematic information that accounts for the upper trunk segment e.g. hip joint angle trajectory can improve the reliability of the ankle regression model. For this reason, it was investigated the effects of combining hip joint angle trajectory with thigh muscles information in data-driven models, tested over long series of strides. In the context of finding a compromise between the simple approach and high performance, the performances of two features sets extracted from the sEMG data were compared. Feature sets are time domain features set (TD) [43], widely adopted in literature, and the Wavelet features set (WT) which has shown high performances in classification purposes [29], [44], [45], [46], [47] and most recently also investigated for regression of joint angles [16]. Machine learning algorithms implemented in this study are Least Squares - Support Vector Machine (LS-SVM) [15], [25], Random Forest (RNF) [48], and Artificial Neural Networks (ANN) [36].

II. Materials and Methods

A. Data Acquisition

An a priori power analysis performed using G*Power software [49] has shown that six subjects with 4 recording sessions would be sufficient to ensure 90% power to detect ($p < 0.05$) a difference in estimated ankle angle using myoelectric data and the latter fused with mechanical data of hip kinematics. Therefore, six non-disabled subjects, 4 females and 2 males, with an age range of 14-50 years, have participated in the experiment. All volunteers were healthy, without any muskuloskeletal, neurological or any other kind of known disease, thus not belonging to vulnerable groups The experimental protocol required that each subject walk back and forth through a 5 m-long path, for a total of 72 gait cycles for each acquisition trial. Each subject performed 4 trials. The experiments were conducted at the Movement Analysis Laboratory of UniversitÃ Politecnica delle Marche (Ancona, Italy), following the Helsinki declaration principles. The equipment used are all commercially available that satisfies technical safety and conformity requirements for clinical applications and involves exclusively non-invasive probes. All the subjects have given their consent to perform the experimental procedure after they have been sufficiently informed about the study goals and methods. All subjects were given enough resting time after each trial and they did not report any stress or muscular fatigue. An alphanumeric code was assigned to each subject and data were stored in an internal repository without any sort of connection to ensure anonymity and confidentiality.

During walking, three sEMG electrodes (FREEE EMG, BTS Bioengineering) were attached to the thigh muscles of the right leg of each subject, following the SENIAM guidelines [50]. The sEMG signals were sampled at 1000 Hz and recorded from Rectus Femoris (RF), Biceps Femoris (BF), and Vastus Medialis (VM). Retroreflective markers were positioned following a full body kinematic protocol [51], which can produce reliable kinematic quantities in the sagittal plane utilizing a minimal number of markers. Their trajectories were captured using 8 infrared cameras system (SMART-DX6000, BTS Bioengineering), recorded at 250 Hz. To avoid inter-examiner variability, the same expert personnel placed the sEMG electrodes and retroreflective markers on each subject.

B. Signal Processing and Feature Extraction

Raw markers data were filtered using a Butterworth 4th order, zero-phase, low pass filter, with a cutoff frequency equal to 9 Hz based on the residual analysis method [52]. Gait epochs were segmented using the vertical component of the right heel marker trajectory. Then, the sagittal plane flexion-extension angle of the hip and ankle joints were reconstructed for each segmented gait epoch, based on retroreflective marker information, following [51]. The sEMG signals from the RF, BF, and VM muscles were segmented in synchronization with the gait epoch data and then were filtered using a Butterworth 2nd order bandpass filter of 10 Hz and 400 Hz cutoff frequencies, respectively. Features were extracted from the sEMG data: TD features include mean absolute value (MAV), root mean square (RMS), and waveform length (WL) [43], [53], [54]. The WT features were energy, variance, standard deviation, waveform length, and entropy [16]. Each of the above-mentioned features was extracted by the outputs of an octave-band filters bank at 5 levels [44], [45], [46], [47] thus having a total of 30 features of each channel of sEMG. Both feature sets were extracted using a window size of 200 ms and sliding increment of 40 ms to have an update rate of 25 Hz [55], [56]. The reason behind selecting these 2 feature sets is to compare the performance of the WT feature set that results in a higher dimensional representation of the myoelectric information at the cost of being more computationally expensive [47], with respect to the light-weight TD feature set that is fast and reliable for real-time applications [43].

Then, kinematic angles of ankle end hip data were downsampled by a factor of 10 to achieve the same update rate of 25 Hz that ensures synchronization with the sEMG-based feature sets. It is worth noticing that this dowsampling factor still guaranteed a proper reconstruction of gait kinematics [52]. The hip angle joint was normalized using Z-score normalization since it's less sensitive to outliers in data distribution [57], [58]. Thus, the normalization of the hip angle was done as in Eq. (1):

$$\theta_n = \frac{\theta - \mu}{\sigma} \tag{1}$$

where θ_n is the normalized hip joint angle, θ is the hip joint angle, μ is the mean of the hip joint angle data from the training sets and σ is its standard deviation. Training and testing hip joint angle data were normalized using the mean and standard deviation calculated from the training set.

The performance of both feature sets were evaluated in a first experiment to assess which was the most reliable for

the purpose of this study. A flowchart of the experimental procedure is reported in Fig. 1.

C. Learning Algorithms

Since the relationship between sEMG features and ankle joint angle is nonlinear, one of the possible solutions is to translate it into a linear regression problem by mapping the input feature space into a higher dimensional space [15], [25], [59]. To this aim, the LS-SVM with a Radial Basis Function (RBF) kernel was employed. The RBF is mathematically expressed as:

$$K(X_i, X_j) = \exp \frac{\left|\left|X_i - X_j\right|\right|^2}{2\sigma^2} \tag{2}$$

where (X_i, X_j) are any input feature vectors and (σ^2) is the kernel parameter which was tuned together with the regularization parameter (γ) of the model in each training trial through Coupled Simulated Annealing (CSA), followed by simplex fine-tuning step and using robust cross-validation score function as an optimization performance measure [60], [61].

In this paper, a single-layer Artificial Neural Network (ANN) with 100 neurons was also applied to compare the results yielded from this shallow model with the other higher-complexity models implemented.

Moreover, random regression trees vectors are used to construct a RNF model through bootstrap re-sampling, such that each random vector (θ_k) is independent and has the same distribution and the tree-structured regression models are $h(x, \theta_k)$, $k = 1, 2, \ldots p$, where x is the input. The predicted value represents the averaged value of $h(x, \theta_k)$ of each tree [48], [62].

D. Regression Experiments

Given the experimental protocol (Section II-A), a 4-fold cross-validation method was implemented: each fold consists of 72 gait cycles thus having a very long series of strides of normal walking for a total of 288 strides for each patient, unlike most of the other previous studies which involved few numbers of strides [20], [25], [36], [63], using a treadmill [25], [63], or performing movements while sitting [25], [48], [64]. The selected validation scheme avoids to expose the models to over-fitting and it guarantees to test the models over a reliable amount of unseen data.

A first regression experiment was carried out to assess which features set between TD and WT provides the best performances among the learning architectures described in section II-C. Hence, for each subject and for each thigh muscle, the models were trained and tested using TD and WT feature sets separately. Furthermore, the contribution of each muscle was also assessed to investigate the existence of minimal and reliable setup configuration.

In the second experiment, the hip angle trajectory was added to sEMG data to overcome any potential underestimation due to using a single not functionally related muscle to the ankle joint. Hence, a minimal hybrid combination between the information from the thigh muscle and a single kinematic variable was assessed by training and testing the learning algorithms. Such models were then compared with those in which kinematic and sEMG data were used separately. The selection of the hip joint angle to be fused with the muscle EMG information was based on the fact that the lower limb joints angles in the sagittal plane are tightly coupled so their relationships can be described by regular loops constrained close to a plane of angular covariation [65], [66], [67]. Therefore, since the hip angle is the only joint angular position variable that is possible to be acquired from the lower limbs in the case of transfemoral amputees, it was included in the input to the data-driven models to evaluate its capability to capture the above-described kinematic relationship without using the knee joint trajectory as an input [20], [21] which does not exist for the latter individuals.

To assess the validity of the minimal sEMG setup, i.e. BF fused with hip trajectory, and to verify the improvement made by the fusion of kinematics with muscle activity, a third regression experiment was carried out. The sEMG features were extracted from the three thigh muscles configurations (3M) and compared with models fed by the same features fused with the hip joint trajectory to investigate the balance of results accuracy and setup complexity when compared to the simpler above-mentioned configurations.

E. Performance Evaluation and Statistical Analysis

The evaluation of the performance of each of the learning models, setup configurations, and features set in each trial is mainly done using 2 parameters which are Root Mean Square Error (RMSE) and Coefficient of Determination (R^2) of the estimated target ankle joint angle that are calculated as the following:

$$\text{RMSE} = \sqrt{\frac{1}{n}\sum_i (\theta_i - \hat{\theta}_i)^2} \tag{3}$$

$$R^2 = 1 - \frac{\sum_i (\theta_i - \hat{\theta}_i)^2}{\sum_i (\theta_i - \bar{\theta})^2} \tag{4}$$

where n is the number of tested samples, θ_i is the actual ankle angle value and $\hat{\theta}_i$ is the estimated ankle angle value.

Further analysis is done using the quantile-quantile (q-q) plot to check if the estimated and actual ankle joint trajectory follow the same distribution thus testing its heteroskedasticity [36]. Also, a plot of the average gait cycle with shaded standard deviation (SD) around for both actual and estimated values is provided to visualize the goodness of fit of the long series of strides in a single figure.

Statistical comparisons were performed by paired t-test (normally distributed data) and Mann-Whitney U-test (not normally distributed data). The significance level was set at 5%. Bonferroni correction for multiple comparisons was applied to handle type I error rates. Cohen's D effect size (d) was also calculated to quantify the significance.

III. Results

A. TD and WT Feature Sets

Table I shows that the RMSE values of the target ankle trajectory estimated from either one of each muscle sEMG

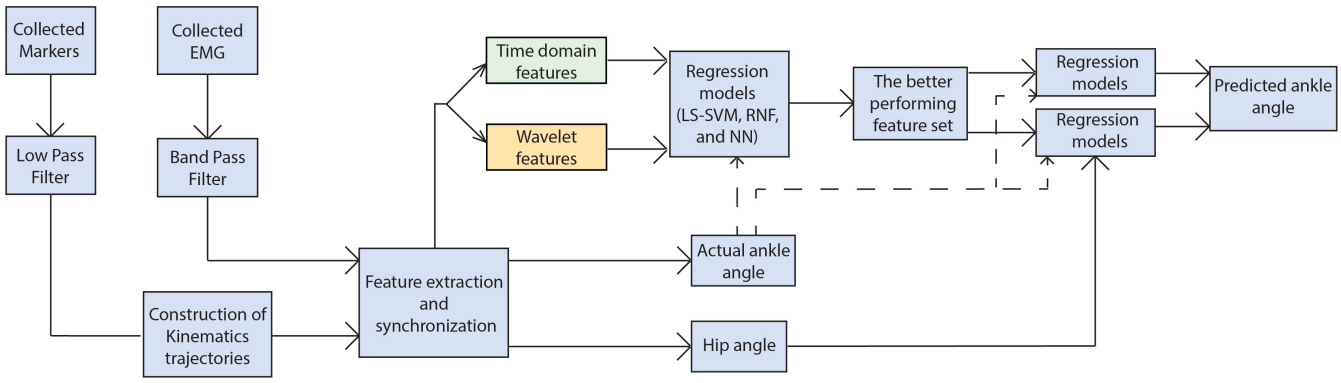

Fig. 1. Methodological procedure for estimating the ankle joint angle. First, ankle joint trajectory was estimated using either time-domain features or wavelet features only. The feature set which showed the best estimation performances has been fused with the hip joint angle for possible improvements. Dashed lines denote data used only in training.

TABLE I

AVERAGE RMSE VALUES (±SD) OF THE ANKLE JOINT ANGLE AMONG ALL THE SUBJECTS ESTIMATED USINGEITHER TD OR WT FEATURE SETS OF THE EMG SIGNAL OF EACH ONE OF THE THIGH MUSCLES (BF, RF, AND VM) USING ALL THE SELECTED MACHINE LEARNINGALGORITHMS (ANN, LS-SVM, AND RNF)

RMSE [deg]	**ANN**		**LS-SVM**		**RNF**	
Muscle	**WT**	**TD**	**WT**	**TD**	**WT**	**TD**
RF	7.11±0.95	6.11±1.03	6.03±0.88	6.06±1.07	6.28±0.89	6.36±1.07
BF	6.25±1.04	5.62±1.13	5.36±0.98	5.56±1.14	5.59±1.04	5.80±1.15
VM	7.08±1.14	6.20±1.22	6.06±1.09	6.18±1.23	6.25±1.12	6.41±1.24

feature sets are close to each other and lie between 5.5 deg and 6.5 deg except for that of the NN model using WT feature set has roughly exceeded 7 deg. Therefore, TD feature set was chosen to proceed the study with.

B. Thigh Muscles

Table I illustrates that the estimation from BF muscle outperformed the use of either one of the other two thigh muscles. In fact, RMSE values for the BF muscle always lie below 6 deg, unlike the other two muscles, whose RMSE was always higher. Confirmation about the goodness of the results can be appreciated in Fig. 2(a) where a graphical comparison between the estimated and actual target ankle angle are viewed for a representative subject.

C. Fusing the EMG Muscles Information With the Hip Kinematic Trajectory

Fig. 3 shows that the RMSE value in the case of the fused input is reduced to nearly about 4.5 deg and below using the three previously mentioned machine learning models. In passing, such RMSE values are lower than those obtained by using only hip angle or BF features.

Then, the RMSE is further reduced into a value of less than 4.0 deg when using the BF, RF, and VM muscles fused with the hip ankle trajectory as input for regression. However, using the same three thigh muscles without adding the hip joint angle led to RMSE well above 4.0 deg (Fig. 4). Improvement made by introducing the hip trajectory in the models on the ankle angle estimation performance are evident also in Fig. 2(b) and Fig. 2(c).

The value of adding hip joint kinematics is further confirmed by the R^2 value, that resulted above 0.6 only when the hip kinematics was considered together with the thigh muscles activity as demonstrated in Fig. 5.

Regarding the different models performances, a comparison between the three machine learning models (ANN, LS-SVM, and RNF) was done for every tested combination of signals. Outcomes reported in Table I, Fig. 3, and Fig. 4 showed a slightly lower RMSE for the LS-SVM with respect to the other models for all of the tested combinations, despite the differences resulted comparable.

IV. DISCUSSION

This paper aims to investigate minimal setup configurations to estimate the flexion-extension ankle joint trajectory in non-constrained gait conditions in a view of possible applicability for transfemoral amputees. Thus, only information from sources all located above the knee joint was employed, i.e. from body structures not directly involved in the flexion-extension of the ankle [3].

The RMSE values obtained using both feature sets (Table I) were nearly at the same level for each thigh muscle, regardless of the regression algorithm. The results reported in the study suggested that in a minimal sEMG setup configuration, only

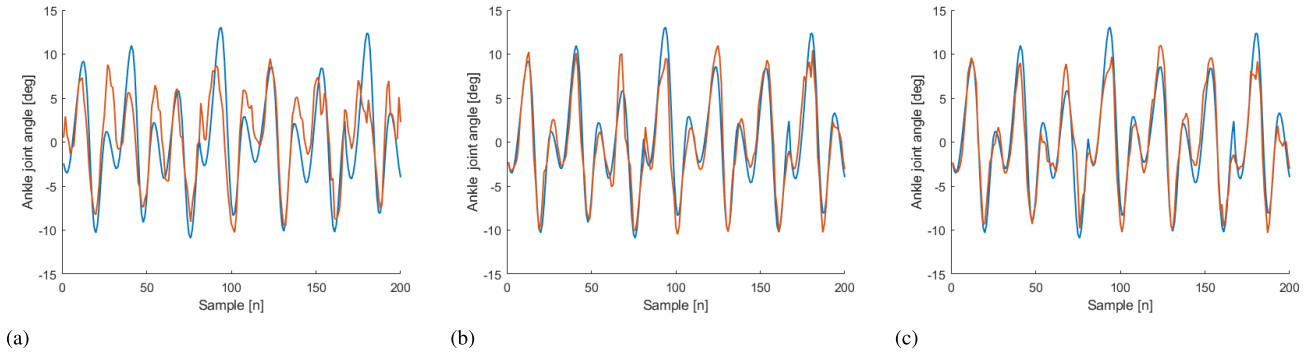

Fig. 2. Actual (blue line) and estimated (orange line) ankle joint trajectories obtained by using only BF features (panel 2(a)), BF features fused with hip joint angle (panel 2(b)), and features from all thigh muscles fused with the hip joint angle (panel 2(c)). In all cases, the LS-SVM regression model was used.

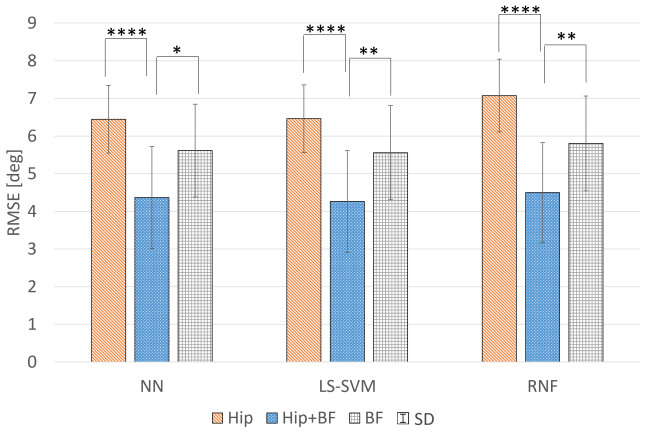

Fig. 3. The average RMSE of the regression with its standard deviation (SD) obtained in the three different conditions as described in Sec. II-D is shown. Asterisks indicate the significance levels as follows: * for ($p < 0.05$), ** for ($p < 0.01$), *** for ($p < 0.001$), and **** for ($p < 0.0001$).

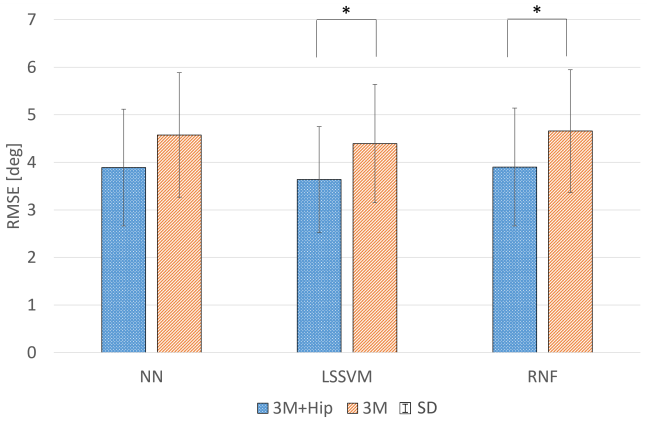

Fig. 4. RMSE of the regression models fed with EMG features from the three thigh muscles (BF, RF, and VM), and with the inclusion of hip joint trajectory.

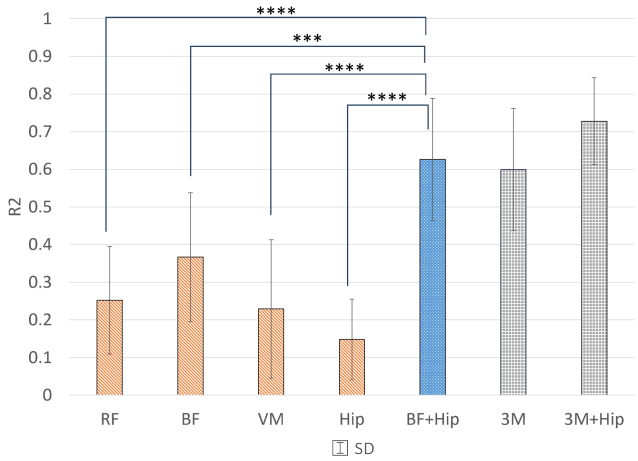

Fig. 5. Averaged R^2 values obtained in testing among subjects for different input combinations by using the LS-SVM model.

a few time descriptors of muscle activity are enough for estimating ankle angle kinematics. It deserves to be noticed that TD features give also computational advantages with respect to more demanding feature extraction procedures, such as those used in time-frequency representation, that provide also a large feature space [44]. This finding does not intersect with previous results as in [16] where it was concluded that regression of TD features outperforms that of WT.

Among the thigh muscles, the BF appeared to be the most informative for the ankle angle estimation since it resulted in significantly lower RMSE (Table I). This is supported also by considering the average Pearson correlation coefficient (r) between the ankle joint angle trajectory and the WL of the three thigh muscles, which resulted in 0.16, 0.09, and 0.33 for VM, RF, and BF respectively, with $p < 0.01$ in each case. Therefore, BF showed the highest correlation with the ankle angle among the examined thigh muscles, highlighting a more phasic behavior with respect to the ankle plantar- dorsi-flexion, even if it is not functionally involved to the ankle kinematics. In passing, the better performances of the BF, with respect to RF and VM, for ankle angle estimation are also highlighted by the R^2, whose BF value resulted the highest among the thigh muscles (Fig. 5). Despite a biomechanical interpretation was beyond the scope of the present work, the role of BF as a predictor of ankle joint kinematics, can be linked to its role as biarticular muscle, that regulates knee flexion and indirectly acts on the ankle thus enhancing a refined regulation of many locomotion functions [68]. Further,

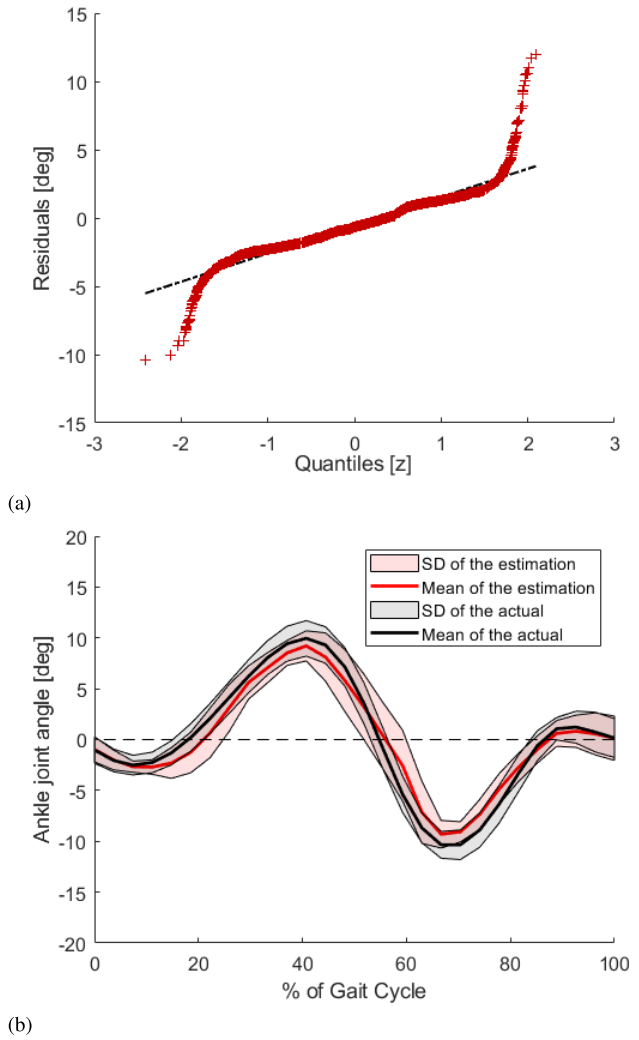

Fig. 6. Panel 6(a) represents the q-q plot of the error residuals for LS-SVM with BF fused with the hip trajectory for a representative subject. Panel 6(b) represents the estimated and real ankle trajectories averaged over the long series of strides. Standard deviations were reported as shadowed areas for both cases.

in a view of practical applicability it deserves to be noted that in TF patients the BF still shows muscular activity that shares common patterns with that of healthy subjects [69], making it a viable zone for recording myoelectric activity after targeted muscle reinnervation [70], [71].

To deal with the possible instability of sEMG signals [3], it was hypothesized that including the kinematic information of the upper part of the lower limb can be beneficial for the ankle angle estimation. Such hypothesis was successfully verified: the addition of the hip joint trajectory to the BF myoelectric activity significantly improved the regression performance with respect to using either BF ($p < 0.001, d = 1.4832$) or hip kinematics alone ($p < 0.0001, d = 3.3204$) (Fig. 3 and Fig. 5). The value of including hip kinematics information is confirmed also by the outcomes obtained when additional thigh muscles were considered. Indeed, also in the latter case, the hip angular trajectory enhanced the ankle angle estimation, by lowering the RMSE below 4.0 deg (Fig. 4). However, it is important to note that, although the 3M+Hip configuration provided the lowest RMSE (Fig. 3 and Fig. 4), it resulted not statistically different ($p > 0.05$) with respect to the BF+Hip configuration, further supporting that BF and hip angular displacement together may represent a reliable minimal setup for predicting ankle joint angular displacement. On one hand, this mirrors previous findings about the improvement of joint angle estimation from myoelectric data by including kinematic information [20], [30], [37], [38]. More importantly, the present outcomes point out that a significant ankle angle estimation enhancement can be obtained also by considering the kinematics of a proximal joint and functionally poorly related with respect to the ankle, such as the hip. This strengthens the possible application of the proposed framework for estimating ankle plantar-dorsi-flexion in individuals who underwent transfemoral amputation, since both myoelectric (BF) and kinematic (Hip) information is still available in this kind of patients. The latter recording configuration represents also a minimal setup that would be attractive in light of an application in real scenarios, being unobtrusive and marginally cumbersome for the patients.

In comparison with other studies that proposed strategies to estimate the ankle angle using data acquired from the upper and lower leg, Mendez et al. [34] yielded during gait an RMSE of 7.39±2.91 deg using ultrasound approach and Zhang et al. [72] achieved an RMSE of 4.22±1.35 deg using sEMG in 20 gait cycles per subject. Furthermore, a deep learning approach using 8 sEMG electrodes yielded RMSE of 3.55±0.23 deg by Lu et al. [16]. In [36] Keleş and Yucesoy found that an RMSE of 2.25±0.34 deg can be achieved using 2 sEMG electrodes from the thigh and one from the shank for a few numbers of gait cycles. Although these studies used directly related and redundant input, the RMSE of 3.64±1.16 deg (Fig. 4) obtained in this study is comparable to their results with the favor of leveraging the predictive myoelectric activity and robust mechanical signals acquired from exclusively above the knee and validated on prolonged sessions using solely machine learning algorithms.

The finding that only a reduced amount of information from the upper part of the lower limb is needed for achieving a reliable ankle kinematics estimation is supported also by considering the average R^2 metric obtained in testing (Fig. 5). LS-SVM model, trained with muscles individually, showed significantly lower values with respect to BF+Hip configuration ($p < 0.0001, d = 2.2769$) for RF and ($p < 0.0001, d = 2.3369$) for VM, indicating that the variance of the testing data is captured in a proper manner when the kinematics is introduced in the model. Furthermore, the R^2 of the 3M and 3M+Hip configurations showed no significantly different values ($p > 0.05, d = 0.1446$) and ($p > 0.05, d = 0.6943$) respectively when compared with the BF+Hip recording setup, indicating once more that the latter can represent a viable minimal configuration for ankle kinematics estimation.

However, for both BF+Hip and 3M+Hip configurations, the R^2 resulted well above 0.60 and 0.70 respectively, pointing out that LS-SVM regression model resulted able to account for the majority of the variance within the testing data, supporting once more the applicability of the proposed solution in an actual scenario.

The consistency between the estimated and real ankle trajectories when using the BF+Hip setup is also supported by considering that the testing estimation residuals resulted to be gaussian (Fig. 6(a)), thus indicating that the estimated and real ankle trajectory have the same distribution. In addition, the data-driven models were also able to mirror the actual evolution of the ankle plantar-dorsi-flexion in terms of pattern variability for prolonged testing trials, showing that real and estimated trajectories follow similar temporal patterns, in terms of both average trajectory and its variance (Fig. 6(b)). The value of present outcomes is also strengthened by considering that in this study the testing phase was performed on over 70 gait cycles, whereas in many similar studies fewer strides were considered [20], [25], [36]. This experimental point was specifically designed in order to resemble closely a real usage application, where the continuous estimation of joint angles during walking has to maintain performance stability for prolonged walking sessions [20], [25], [36].

The attention provided to the practical usability of the proposed minimal setup (BF+Hip) can be recognized also in the fact that this work focused on natural, unconstrained gait to have similar to real-world variability conditions which represents a significant difference with respect to many previous studies, where the proposed lower limb angular estimation solutions were tested in more controlled contexts, such as constrained speed [11] or treadmill walking [73], that naturally leads to constrained muscle activation profiles [74]. On the other hand, recent works in literature highlighted the importance of different ambulation modes i.e. ramps, or stairs in prosthetic control [16], [73], indicating that future studies should be devoted to the generalization of the proposed minimal setup machine-learning framework for different gait modalities. A possible approach could be done by training on a range of movements and assessing the model's capability to generalize to a new locomotion mode that was not included within the training data, that represents a still poorly investigated field for the advancements of the prosthetic control. Other future research can also be devoted to the generalization of the proposed solution to multiple users to develop a multi-user architecture for myoelectric control of joint kinematics.

This paper has some limitations that deserve to be briefly discussed. Firstly, experimental evaluations have been developed on intact individuals who may have different myoelectric characteristics with respect to that of non-intact subjects. Hence, findings of this study should be further tested on impaired patients in order to confirm their suitability for controlling lower limb assistive devices. In addition, hip angular kinematics has been attained by using an optoelectronic system, that would be not directly applicable in daily living scenarios. Thus, this requires further investigation about the validity of the proposed methodology when hip kinematics is recorded by means of inertial sensors, that do not require instrumented environments [75], [76], [77]. Lastly, due to the complex relationship between the myoelectric activity and the kinematics variables, recent works [11], [16] have used deep learning models to boost the estimation performance but at the expense of higher computational load. However, their results are still comparable to the results of the machine-learning approaches adopted in this paper. Additionally, a final point that deserves to be mentioned regards the comparison of data driven models with physical based ones, that represents a promising research avenue, since in recent studies data-driven approaches were directly compared with biomechanical models, showing consistent performances also over consecutive days [78].

V. Conclusion

In this work, a minimal recording setup was proposed for the estimation of ankle kinematics during walking. In particular, it has been shown that a single sEMG probe located on a functionally unrelated muscle, such as the BF, provided good results in terms of flexion-extension reconstruction. The latter was further enhanced by the inclusion of the hip joint angular trajectory. Thus, results of this study can be seen as a first step toward the development of practical solutions for driving prosthetic and rehabilitative devices for the ankle joint, representing a potentially valuable solution for those individuals who underwent TF amputation, since the required information would be still available in this kind of patients. Practical applicability was also emphasized by the stability of the estimation obtained in testing, where more than 70 consecutive strides were considered, mirroring a free walking scenario in an actual environment.

References

[1] P. W. Moxey et al., "Lower extremity amputations—A review of global variability in incidence," *Diabetic Med.*, vol. 28, no. 10, pp. 1144–1153, Oct. 2011.

[2] C. L. McDonald, S. Westcott-McCoy, M. R. Weaver, J. Haagsma, and D. Kartin, "Global prevalence of traumatic non-fatal limb amputation," *Prosthetics Orthotics Int.*, vol. 45, no. 2, pp. 105–114, 2021.

[3] B. Ahkami, K. Ahmed, A. Thesleff, L. Hargrove, and M. Ortiz-Catalan, "Electromyography-based control of lower limb prostheses: A systematic review," *IEEE Trans. Med. Robot. Bionics*, vol. 5, no. 3, pp. 547–562, Aug. 2023.

[4] M. Windrich, M. Grimmer, O. Christ, S. Rinderknecht, and P. Beckerle, "Active lower limb prosthetics: A systematic review of design issues and solutions," *Biomed. Eng. OnLine*, vol. 15, no. S3, pp. 5–19, Dec. 2016.

[5] C. Fanciullacci et al., "Survey of transfemoral amputee experience and priorities for the user-centered design of powered robotic transfemoral prostheses," *J. Neuroeng. Rehabil.*, vol. 18, no. 1, pp. 1–25, Dec. 2021.

[6] N. Wolfson, "Amputations in natural disasters and mass casualties: Staged approach," *Int. Orthopaedics*, vol. 36, no. 10, pp. 1983–1988, Oct. 2012.

[7] R. Gehlhar, M. Tucker, A. J. Young, and A. D. Ames, "A review of current state-of-the-art control methods for lower-limb powered prostheses," *Annu. Rev. Control*, vol. 55, pp. 142–164, Jan. 2023.

[8] B. S. Rupal, S. Rafique, A. Singla, E. Singla, M. Isaksson, and G. S. Virk, "Lower-limb exoskeletons: Research trends and regulatory guidelines in medical and non-medical applications," *Int. J. Adv. Robotic Syst.*, vol. 14, no. 6, 2017, Art. no. 1729881417743554.

[9] S. Maggioni et al., "Robot-aided assessment of lower extremity functions: A review," *J. Neuroeng. Rehabil.*, vol. 13, no. 1, pp. 1–25, Dec. 2016.

[10] A. S. Ciullo et al., "A novel soft robotic supernumerary hand for severely affected stroke patients," *IEEE Trans. Neural Syst. Rehabil. Eng.*, vol. 28, no. 5, pp. 1168–1177, May 2020.

[11] J. Chen, X. Zhang, Y. Cheng, and N. Xi, "Surface EMG based continuous estimation of human lower limb joint angles by using deep belief networks," *Biomed. Signal Process. Control*, vol. 40, pp. 335–342, Feb. 2018.

[12] M. Eslamy and K. Alipour, "Synergy-based Gaussian process estimation of ankle angle and torque: Conceptualization for high level controlling of active robotic foot prostheses/orthoses," *J. Biomech. Eng.*, vol. 141, no. 2, Feb. 2019.

[13] N. Nazmi, M. A. Abdul Rahman, S.-I. Yamamoto, and S. A. Ahmad, "Walking gait event detection based on electromyography signals using artificial neural network," *Biomed. Signal Process. Control*, vol. 47, pp. 334–343, Jan. 2019.

[14] L. Zhang, Z. Li, Y. Hu, C. Smith, E. M. G. Farewik, and R. Wang, "Ankle joint torque estimation using an EMG-driven neuromusculoskeletal model and an artificial neural network model," *IEEE Trans. Autom. Sci. Eng.*, vol. 18, no. 2, pp. 564–573, Apr. 2021.

[15] Z. Sun, X. Zhang, K. Liu, T. Shi, and J. Wang, "A multi-joint continuous motion estimation method of lower limb using least squares support vector machine and zeroing neural network based on sEMG signals," *Neural Process. Lett.*, vol. 55, no. 3, pp. 2867–2884, Jun. 2023.

[16] Y. Lu, H. Wang, B. Zhou, C. Wei, and S. Xu, "Continuous and simultaneous estimation of lower limb multi-joint angles from sEMG signals based on stacked convolutional and LSTM models," *Expert Syst. Appl.*, vol. 203, Oct. 2022, Art. no. 117340.

[17] A. Buniya, A. H. Al-Timemy, A. Aldoori, and R. N. Khushaba, "Analysis of different hand and finger grip patterns using surface electromyography and hand dynamometry," *Al-Khwarizmi Eng. J.*, vol. 16, no. 2, pp. 14–23, Jun. 2020.

[18] H. Huang, F. Zhang, L. J. Hargrove, Z. Dou, D. R. Rogers, and K. B. Englehart, "Continuous locomotion-mode identification for prosthetic legs based on neuromuscular–mechanical fusion," *IEEE Trans. Biomed. Eng.*, vol. 58, no. 10, pp. 2867–2875, Oct. 2011.

[19] I. S. Dhindsa, R. Agarwal, and H. S. Ryait, "Principal component analysis-based muscle identification for myoelectric-controlled exoskeleton knee," *J. Appl. Statist.*, vol. 44, no. 10, pp. 1707–1720, Jul. 2017.

[20] R. Gupta, I. S. Dhindsa, and R. Agarwal, "Continuous angular position estimation of human ankle during unconstrained locomotion," *Biomed. Signal Process. Control*, vol. 60, Jul. 2020, Art. no. 101968.

[21] S. Dey, M. Eslamy, T. Yoshida, M. Ernst, T. Schmalz, and A. F. Schilling, "A support vector regression approach for continuous prediction of ankle angle and moment during walking: An implication for developing a control strategy for active ankle prostheses," in *Proc. IEEE 16th Int. Conf. Rehabil. Robot. (ICORR)*, Jun. 2019, pp. 727–733.

[22] C. P. Cop, G. Durandau, A. M. Esteban, R. C. van 't Veld, A. C. Schouten, and M. Sartori, "Model-based estimation of ankle joint stiffness during dynamic tasks: A validation-based approach," in *Proc. 41st Annu. Int. Conf. IEEE Eng. Med. Biol. Soc. (EMBC)*, Jul. 2019, pp. 4104–4107.

[23] U. Mamikoglu, G. Andrikopoulos, G. Nikolakopoulos, U. Röijezon, M. Pauelsen, and T. Gustafsson, "Electromyography based joint angle estimation and control of a robotic leg," in *Proc. 6th IEEE Int. Conf. Biomed. Robot. Biomechatronics (BioRob)*, Jun. 2016, pp. 182–187.

[24] C. Fleischer and G. Hommel, "A human–exoskeleton interface utilizing electromyography," *IEEE Trans. Robot.*, vol. 24, no. 4, pp. 872–882, Aug. 2008.

[25] Q. L. Li, Y. Song, and Z. G. Hou, "Estimation of lower limb periodic motions from sEMG using least squares support vector regression," *Neural Process. Lett.*, vol. 41, no. 3, pp. 371–388, Jun. 2015.

[26] F. Zhang et al., "sEMG-based continuous estimation of joint angles of human legs by using BP neural network," *Neurocomputing*, vol. 78, no. 1, pp. 139–148, Feb. 2012.

[27] T. Lee, I. Kim, and S.-H. Lee, "Estimation of the continuous walking angle of knee and ankle (talocrural joint, subtalar joint) of a lower-limb exoskeleton robot using a neural network," *Sensors*, vol. 21, no. 8, p. 2807, Apr. 2021.

[28] T. Afzal, K. Iqbal, G. White, and A. B. Wright, "A method for locomotion mode identification using muscle synergies," *IEEE Trans. Neural Syst. Rehabil. Eng.*, vol. 25, no. 6, pp. 608–617, Jun. 2017.

[29] K. Englehart, B. Hudgin, and P. A. Parker, "A wavelet-based continuous classification scheme for multifunction myoelectric control," *IEEE Trans. Biomed. Eng.*, vol. 48, no. 3, pp. 302–311, Mar. 2001.

[30] F. Zhang and H. Huang, "Source selection for real-time user intent recognition toward volitional control of artificial legs," *IEEE J. Biomed. Health Informat.*, vol. 17, no. 5, pp. 907–914, Sep. 2013.

[31] J. Liu, S. H. Kang, D. Xu, Y. Ren, S. J. Lee, and L.-Q. Zhang, "EMG-based continuous and simultaneous estimation of arm kinematics in able-bodied individuals and stroke survivors," *Front. Neurosci.*, vol. 11, p. 480, Aug. 2017.

[32] F.-G. Meng, B. Zhang, X.-G. Zhao, and J. Sui, "Estimation of ankle joint continuous motion based on electromyographic signals," in *Proc. Chin. Autom. Congr. (CAC)*, Nov. 2020, pp. 6399–6406.

[33] A. H. Al-Timemy, A. Zonnino, and F. Sergi, "Estimating wrist joint torque using regression ensemble of bagged trees under multiple wrist postures," in *Proc. 8th IEEE RAS/EMBS Int. Conf. for Biomed. Robot. Biomechatronics (BioRob)*, Nov. 2020, pp. 1152–1157.

[34] J. Mendez, R. Murray, L. Gabert, N. P. Fey, H. Liu, and T. Lenzi, "A-mode ultrasound-based prediction of transfemoral amputee prosthesis walking kinematics via an artificial neural network," *IEEE Trans. Neural Syst. Rehabil. Eng.*, vol. 31, pp. 1511–1520, 2023.

[35] T. Liang et al., "SEMG-based end-to-end continues prediction of human knee joint angles using the tightly coupled convolutional transformer model," *IEEE J. Biomed. Health Informat.*, vol. 27, no. 11, pp. 5272–5280, Nov. 2023.

[36] A. D. Keleş and C. A. Yucesoy, "Development of a neural network based control algorithm for powered ankle prosthesis," *J. Biomech.*, vol. 113, Dec. 2020, Art. no. 110087.

[37] J. A. Spanias, A. M. Simon, K. A. Ingraham, and L. J. Hargrove, "Effect of additional mechanical sensor data on an EMG-based pattern recognition system for a powered leg prosthesis," in *Proc. Int. IEEE/EMBS Conf. Neural Eng. (NER)*, Jul. 2015, pp. 639–642.

[38] A. J. Young, T. A. Kuiken, and L. J. Hargrove, "Analysis of using EMG and mechanical sensors to enhance intent recognition in powered lower limb prostheses," *J. Neural Eng.*, vol. 11, no. 5, Oct. 2014, Art. no. 056021.

[39] A. Cimolato, J. J. M. Driessen, L. S. Mattos, E. De Momi, M. Laffranchi, and L. De Michieli, "EMG-driven control in lower limb prostheses: A topic-based systematic review," *J. Neuroeng. Rehabil.*, vol. 19, no. 1, pp. 1–26, 2022.

[40] R. Jiménez-Fabián and O. Verlinden, "Review of control algorithms for robotic ankle systems in lower-limb orthoses, prostheses, and exoskeletons," *Med. Eng. Phys.*, vol. 34, no. 4, pp. 397–408, May 2012.

[41] A. J. Young and D. P. Ferris, "State of the art and future directions for lower limb robotic exoskeletons," *IEEE Trans. Neural Syst. Rehabil. Eng.*, vol. 25, no. 2, pp. 171–182, Feb. 2017.

[42] S. K. Au, P. Bonato, and H. Herr, "An EMG-position controlled system for an active ankle-foot prosthesis: An initial experimental study," in *Proc. IEEE Int. Conf. Rehabil. Robot.*, Jun. 2005, pp. 375–379.

[43] S. Micera, J. Carpaneto, and S. Raspopovic, "Control of hand prostheses using peripheral information," *IEEE Rev. Biomed. Eng.*, vol. 3, pp. 48–68, 2010.

[44] R. N. Khushaba, A. Al-Jumaily, and A. Al-Ani, "Novel feature extraction method based on fuzzy entropy and wavelet packet transform for myoelectric control," in *Proc. Int. Symp. Commun. Inf. Technol.*, Oct. 2007, pp. 352–357.

[45] R. N. Khushaba, S. Kodagoda, S. Lal, and G. Dissanayake, "Driver drowsiness classification using fuzzy wavelet-packet-based feature-extraction algorithm," *IEEE Trans. Biomed. Eng.*, vol. 58, no. 1, pp. 121–131, Jan. 2011.

[46] A. H. Al-Timemy, Y. Serrestou, R. N. Khushaba, S. Yacoub, and K. Raoof, "Hand gesture recognition with acoustic myography and wavelet scattering transform," *IEEE Access*, vol. 10, pp. 107526–107535, 2022.

[47] J.-U. Chu, I. Moon, S.-K. Kim, and M.-S. Mun, "Control of multifunction myoelectric hand using a real-time EMG pattern recognition," in *Proc. IEEE/RSJ Int. Conf. Intell. Robots Syst.*, Aug. 2005, pp. 3511–3516.

[48] C. Huihui, G. Farong, C. Chao, and T. Taixing, "Estimation of ankle angle based on multi-feature fusion with random forest," in *Proc. 37th Chin. Control Conf. (CCC)*, Jul. 2018, pp. 5549–5553.

[49] F. Faul, E. Erdfelder, A.-G. Lang, and A. Buchner, "G*Power 3: A flexible statistical power analysis program for the social, behavioral, and biomedical sciences," *Behav. Res. Methods*, vol. 39, no. 2, pp. 175–191, May 2007.

[50] H. J. Hermens, B. Freriks, C. Disselhorst-Klug, and G. Rau, "Development of recommendations for SEMG sensors and sensor placement procedures," *J. Electromyogr. Kinesiol.*, vol. 10, no. 5, pp. 361–374, 2000.

[51] R. B. Davis, S. Ounpuu, D. Tyburski, and J. R. Gage, "A gait analysis data collection and reduction technique," *Human Movement Sci.*, vol. 10, pp. 575–587, Oct. 1991.

[52] D. A. Winter, *Biomechanics and Motor Control of Human Movement*. Hoboken, NJ, USA: Wiley, 2009.

[53] A. Tigrini et al., "Decoding transient sEMG data for intent motion recognition in transhumeral amputees," *Biomed. Signal Process. Control*, vol. 85, Aug. 2023, Art. no. 104936.

[54] A. Mengarelli et al., "Toward a minimal sEMG setup for knee and ankle kinematic estimation during gait," in *Proc. IEEE 36th Int. Symp. Comput.-Based Med. Syst. (CBMS)*, Jun. 2023, pp. 293–298.

[55] Z. Li, B. Wang, F. Sun, C. Yang, Q. Xie, and W. Zhang, "SEMG-based joint force control for an upper-limb power-assist exoskeleton robot," *IEEE J. Biomed. Health Informat.*, vol. 18, no. 3, pp. 1043–1050, May 2014.

[56] Z. Lu, X. Chen, X. Zhang, K.-Y. Tong, and P. Zhou, "Real-time control of an exoskeleton hand robot with myoelectric pattern recognition," *Int. J. Neural Syst.*, vol. 27, no. 5, Aug. 2017, Art. no. 1750009.

[57] R. Tanawongsuwan and A. Bobick, "Gait recognition from time-normalized joint-angle trajectories in the walking plane," in *Proc. IEEE Comput. Soc. Conf. Comput. Vis. Pattern Recognit. (CVPR)*, vol. 2, Dec. 2001, pp. 11726–11731.

[58] J. Han, M. Kamber, and J. Pei, *Data Mining Concepts and Techniques*, 3rd ed. Urbana, IL, USA: Univ. Illinois, 2012.

[59] J. A. K. Suykens and J. Vandewalle, "Least squares support vector machine classifiers," *Neural Process. Lett.*, vol. 9, no. 1, pp. 293–300, 1999.

[60] J. De Brabanter, K. Pelckmans, J. A. Suykens, and J. Vandewalle, "Robust cross-validation score function for non-linear function estimation," in *Proc. Int. Conf. Artif. Neural Netw. (ICANN)*, Madrid, Spain. Springer, Aug. 2002, pp. 713–719.

[61] S. Xavier-de-Souza, J. A. K. Suykens, J. Vandewalle, and D. Bolle, "Coupled simulated annealing," *IEEE Trans. Syst., Man, Cybern. B, Cybern.*, vol. 40, no. 2, pp. 320–335, Apr. 2010.

[62] L. Breiman, "Random forests," *Mach. Learn.*, vol. 45, pp. 5–32, Oct. 2001.

[63] C. Cui, G. B. Bian, Z. G. Hou, X. L. Xie, L. Peng, and D. Zhang, "SEMG-based prediction of human lower extremity movements by using a dynamic recurrent neural network," in *Proc. 28th Chin. Control Decis. Conf. (CCDC)*, 2016, pp. 5021–5026.

[64] M. T. N. Truong, A. E. A. Ali, D. Owaki, and M. Hayashibe, "EMG-based estimation of lower limb joint angles and moments using long short-term memory network," *Sensors*, vol. 23, no. 6, p. 3331, 2023.

[65] F. Lacquaniti, R. Grasso, and M. Zago, "Motor patterns in walking," *Physiology*, vol. 14, no. 4, pp. 168–174, Aug. 1999.

[66] J. A. Walsh, A. Stamenkovic, J. P. Dawber, and P. J. Stapley, "Use of planar covariation in lower limb kinematics to characterize adaptations of running after cycling in elite triathletes," *Frontiers Sports Act. Living*, vol. 4, Jan. 2023, Art. no. 1047369.

[67] Y. P. Ivanenko, A. d'Avella, R. E. Poppele, and F. Lacquaniti, "On the origin of planar covariation of elevation angles during human locomotion," *J. Neurophysiology*, vol. 99, no. 4, pp. 1890–1898, Apr. 2008.

[68] M. A. Sharbafi, H. Barazesh, M. Iranikhah, and A. Seyfarth, "Leg force control through biarticular muscles for human walking assistance," *Frontiers Neurorobotics*, vol. 12, p. 39, Jul. 2018.

[69] E. C. Wentink, E. C. Prinsen, J. S. Rietman, and P. H. Veltink, "Comparison of muscle activity patterns of transfemoral amputees and control subjects during walking," *J. Neuroeng. Rehabil.*, vol. 10, no. 1, p. 87, 2013.

[70] T. A. Kuiken, A. K. Barlow, L. J. Hargrove, and G. A. Dumanian, "Targeted muscle reinnervation for the upper and lower extremity," *Techn. Orthopaedics*, vol. 32, no. 2, pp. 109–116, 2017.

[71] S. P. Agnew, A. E. Schultz, G. A. Dumanian, and T. A. Kuiken, "Targeted reinnervation in the transfemoral amputee: A preliminary study of surgical technique," *Plastic Reconstructive Surg.*, vol. 129, no. 1, pp. 187–194, Jan. 2012.

[72] Q. Zhang, A. Iyer, Z. Sun, K. Kim, and N. Sharma, "A dual-modal approach using electromyography and sonomyography improves prediction of dynamic ankle movement: A case study," *IEEE Trans. Neural Syst. Rehabil. Eng.*, vol. 29, pp. 1944–1954, 2021.

[73] X. Zhou, C. Wang, L. Zhang, J. Liu, G. Liang, and X. Wu, "Continuous estimation of lower limb joint angles from multi-stream signals based on knowledge tracing," *IEEE Robot. Autom. Lett.*, vol. 8, no. 2, pp. 951–957, Feb. 2023.

[74] I. Mileti et al., "Muscle activation patterns are more constrained and regular in treadmill than in overground human locomotion," *Frontiers Bioeng. Biotechnol.*, vol. 8, Oct. 2020, Art. no. 581619. [Online]. Available: https://www.frontiersin.org/articles/10.3389/fbioe.2020.581619

[75] S. Cerfoglio et al., "Evaluation of upper body and lower limbs kinematics through an IMU-based medical system: A comparative study with the optoelectronic system," *Sensors*, vol. 23, no. 13, p. 6156, Jul. 2023.

[76] L. Chia, J. T. Andersen, M. J. McKay, J. Sullivan, T. Megalaa, and E. Pappas, "Evaluating the validity and reliability of inertial measurement units for determining knee and trunk kinematics during athletic landing and cutting movements," *J. Electromyogr. Kinesiol.*, vol. 60, Oct. 2021, Art. no. 102589.

[77] S. Ciklacandir, S. Ozkan, and Y. Isler, "A comparison of the performances of video-based and IMU sensor-based motion capture systems on joint angles," in *Proc. Innov. Intell. Syst. Appl. Conf. (ASYU)*, Sep. 2022, pp. 1–5.

[78] R. V. Schulte, M. Zondag, J. H. Buurke, and E. C. Prinsen, "Multi-day EMG-based knee joint torque estimation using hybrid neuromusculoskeletal modelling and convolutional neural networks," *Frontiers Robot. AI*, vol. 9, Apr. 2022, Art. no. 869476.